

This is the accepted manuscript made available via CHORUS. The article has been published as:

Study of substructure of high transverse momentum jets
produced in proton-antiproton collisions at
 $\sqrt{s}=1.96$ TeV

T. Aaltonen *et al.* (CDF Collaboration)

Phys. Rev. D **85**, 091101 — Published 3 May 2012

DOI: [10.1103/PhysRevD.85.091101](https://doi.org/10.1103/PhysRevD.85.091101)

Study of Substructure of High Transverse Momentum Jets Produced in Proton-Antiproton Collisions at $\sqrt{s} = 1.96$ TeV

T. Aaltonen,²¹ R. Alon^z,³¹ B. Álvarez González^w,⁹ S. Amerio,⁴¹ D. Amidei,³²
A. Anastassov,³⁶ A. Annovi,¹⁷ J. Antos,¹² G. Apollinari,¹⁵ J.A. Appel,¹⁵ A. Apresyan,⁴⁶
T. Arisawa,⁵⁶ A. Artikov,¹³ J. Asaadi,⁵¹ W. Ashmanskas,¹⁵ B. Auerbach,⁵⁹ A. Aurisano,⁵¹
F. Azfar,⁴⁰ W. Badgett,¹⁵ A. Barbaro-Galtieri,²⁶ V.E. Barnes,⁴⁶ B.A. Barnett,²³
P. Barria^{dd},⁴⁴ P. Bartos,¹² M. Bauce^{bb},⁴¹ G. Bauer,³⁰ F. Bedeschi,⁴⁴ D. Beecher,²⁸
S. Behari,²³ G. Bellettini^{cc},⁴⁴ J. Bellinger,⁵⁸ D. Benjamin,¹⁴ A. Beretvas,¹⁵ A. Bhatti,⁴⁸
M. Binkley^a,¹⁵ D. Bisello^{bb},⁴¹ I. Bizjak^{hh},²⁸ K.R. Bland,⁵ B. Blumenfeld,²³ A. Bocci,¹⁴
A. Bodek,⁴⁷ D. Bortoletto,⁴⁶ J. Boudreau,⁴⁵ A. Boveia,¹¹ L. Brigliadori^{aa},⁶ A. Brisuda,¹²
C. Bromberg,³³ E. Brucken,²¹ M. Bucciantonio^{cc},⁴⁴ J. Budagov,¹³ H.S. Budd,⁴⁷
S. Budd,²² K. Burkett,¹⁵ G. Busetto^{bb},⁴¹ P. Bussey,¹⁹ A. Buzatu,³¹ C. Calancha,²⁹
S. Camarda,⁴ M. Campanelli,²⁸ M. Campbell,³² F. Canelli¹¹,¹⁵ B. Carls,²² D. Carlsmith,⁵⁸
R. Carosi,⁴⁴ S. Carrillo^k,¹⁶ S. Carron,¹⁵ B. Casal,⁹ M. Casarsa,¹⁵ A. Castro^{aa},⁶
P. Catastini,²⁰ D. Cauz,⁵² V. Cavaliere,²² M. Cavalli-Sforza,⁴ A. Cerri^e,²⁶ L. Cerrito^q,²⁸
Y.C. Chen,¹ M. Chertok,⁷ G. Chiarelli,⁴⁴ G. Chlachidze,¹⁵ F. Chlebana,¹⁵ K. Cho,²⁵
D. Chokheli,¹³ J.P. Chou,²⁰ W.H. Chung,⁵⁸ Y.S. Chung,⁴⁷ C.I. Ciobanu,⁴² M.A. Ciocchi^{dd},⁴⁴
A. Clark,¹⁸ C. Clarke,⁵⁷ G. Compostella^{bb},⁴¹ M.E. Convery,¹⁵ J. Conway,⁷ M. Corbo,⁴²
M. Cordelli,¹⁷ C.A. Cox,⁷ D.J. Cox,⁷ F. Crescioli^{cc},⁴⁴ C. Cuenca Almenar,⁵⁹ J. Cuevas^w,⁹
R. Culbertson,¹⁵ D. Dagenhart,¹⁵ N. d'Ascenzo^u,⁴² M. Datta,¹⁵ P. de Barbaro,⁴⁷
S. De Cecco,⁴⁹ G. De Lorenzo,⁴ M. Dell'Orso^{cc},⁴⁴ C. Deluca,⁴ L. Demortier,⁴⁸
J. Deng^b,¹⁴ M. Deninno,⁶ F. Devoto,²¹ M. d'Errico^{bb},⁴¹ A. Di Canto^{cc},⁴⁴ B. Di Ruzza,⁴⁴
J.R. Dittmann,⁵ M. D'Onofrio,²⁷ S. Donati^{cc},⁴⁴ P. Dong,¹⁵ M. Dorigo,⁵² T. Dorigo,⁴¹
E. Duchovni^z,³¹ K. Ebina,⁵⁶ A. Elagin,⁵¹ A. Eppig,³² R. Erbacher,⁷ D. Errede,²²
S. Errede,²² N. Ershaidat^{aa},⁴² R. Eusebi,⁵¹ H.C. Fang,²⁶ S. Farrington,⁴⁰ M. Feindt,²⁴
J.P. Fernandez,²⁹ C. Ferrazza^{ee},⁴⁴ R. Field,¹⁶ G. Flanagan^s,⁴⁶ R. Forrest,⁷ M.J. Frank,⁵
M. Franklin,²⁰ J.C. Freeman,¹⁵ Y. Funakoshi,⁵⁶ I. Furic,¹⁶ M. Gallinaro,⁴⁸ J. Galyardt,¹⁰
J.E. Garcia,¹⁸ A.F. Garfinkel,⁴⁶ P. Garosi^{dd},⁴⁴ H. Gerberich,²² E. Gerchtein,¹⁵ S. Giagu^{ff},⁴⁹
V. Giakoumopoulou,³ P. Giannetti,⁴⁴ K. Gibson,⁴⁵ C.M. Ginsburg,¹⁵ N. Giokaris,³

^a Deceased

P. Giromini,¹⁷ M. Giunta,⁴⁴ G. Giurgiu,²³ V. Glagolev,¹³ D. Glenzinski,¹⁵ M. Gold,³⁵
 D. Goldin,⁵¹ N. Goldschmidt,¹⁶ A. Golossanov,¹⁵ G. Gomez,⁹ G. Gomez-Ceballos,³⁰
 M. Goncharov,³⁰ O. González,²⁹ I. Gorelov,³⁵ A.T. Goshaw,¹⁴ K. Goulianos,⁴⁸ S. Grinstein,⁴
 C. Grosso-Pilcher,¹¹ R.C. Group^{55,15} J. Guimaraes da Costa,²⁰ Z. Gunay-Unalan,³³
 C. Haber,²⁶ S.R. Hahn,¹⁵ E. Halkiadakis,⁵⁰ A. Hamaguchi,³⁹ J.Y. Han,⁴⁷ F. Happacher,¹⁷
 K. Hara,⁵³ D. Hare,⁵⁰ M. Hare,⁵⁴ R.F. Harr,⁵⁷ K. Hatakeyama,⁵ C. Hays,⁴⁰ M. Heck,²⁴
 J. Heinrich,⁴³ M. Herndon,⁵⁸ S. Hewamanage,⁵ D. Hidas,⁵⁰ A. Hocker,¹⁵ W. Hopkins^{f,15}
 D. Horn,²⁴ S. Hou,¹ R.E. Hughes,³⁷ M. Hurwitz,¹¹ U. Husemann,⁵⁹ N. Hussain,³¹
 M. Hussein,³³ J. Huston,³³ G. Introzzi,⁴⁴ M. Iori^{ff,49} A. Ivanov^{o,7} E. James,¹⁵ D. Jang,¹⁰
 B. Jayatilaka,¹⁴ E.J. Jeon,²⁵ M.K. Jha,⁶ S. Jindariani,¹⁵ W. Johnson,⁷ M. Jones,⁴⁶
 K.K. Joo,²⁵ S.Y. Jun,¹⁰ T.R. Junk,¹⁵ T. Kamon,⁵¹ P.E. Karchin,⁵⁷ A. Kasmi,⁵ Y. Kato^{n,39}
 W. Ketchum,¹¹ J. Keung,⁴³ V. Khotilovich,⁵¹ B. Kilminster,¹⁵ D.H. Kim,²⁵ H.S. Kim,²⁵
 H.W. Kim,²⁵ J.E. Kim,²⁵ M.J. Kim,¹⁷ S.B. Kim,²⁵ S.H. Kim,⁵³ Y.K. Kim,¹¹ N. Kimura,⁵⁶
 M. Kirby,¹⁵ S. Klimenko,¹⁶ K. Kondo,⁵⁶ D.J. Kong,²⁵ J. Konigsberg,¹⁶ A.V. Kotwal,¹⁴
 M. Kreps,²⁴ J. Kroll,⁴³ D. Krop,¹¹ N. Krumnack^{l,5} M. Kruse,¹⁴ V. Krutelyov^{c,51} T. Kuhr,²⁴
 M. Kurata,⁵³ S. Kwang,¹¹ A.T. Laasanen,⁴⁶ S. Lami,⁴⁴ S. Lammel,¹⁵ M. Lancaster,²⁸
 R.L. Lander,⁷ K. Lannon^{v,37} A. Lath,⁵⁰ G. Latino^{cc,44} T. LeCompte,² E. Lee,⁵¹ H.S. Lee,¹¹
 J.S. Lee,²⁵ S.W. Lee^{x,51} S. Leo^{cc,44} S. Leone,⁴⁴ J.D. Lewis,¹⁵ A. Limosani^{r,14} C.-J. Lin,²⁶
 J. Linacre,⁴⁰ M. Lindgren,¹⁵ E. Lipeles,⁴³ A. Lister,¹⁸ D.O. Litvintsev,¹⁵ C. Liu,⁴⁵
 Q. Liu,⁴⁶ T. Liu,¹⁵ S. Lockwitz,⁵⁹ A. Loginov,⁵⁹ D. Lucchesi^{bb,41} J. Lueck,²⁴ P. Lujan,²⁶
 P. Lukens,¹⁵ G. Lungu,⁴⁸ J. Lys,²⁶ R. Lysak,¹² R. Madrak,¹⁵ K. Maeshima,¹⁵
 K. Makhoul,³⁰ S. Malik,⁴⁸ G. Manca^{a,27} A. Manousakis-Katsikakis,³ F. Margaroli,⁴⁶
 C. Marino,²⁴ M. Martínez,⁴ R. Martínez-Ballarín,²⁹ P. Mastrandrea,⁴⁹ M.E. Mattson,⁵⁷
 P. Mazzanti,⁶ K.S. McFarland,⁴⁷ P. McIntyre,⁵¹ R. McNulty^{i,27} A. Mehta,²⁷ P. Mehtala,²¹
 A. Menzione,⁴⁴ C. Mesropian,⁴⁸ T. Miao,¹⁵ D. Mietlicki,³² A. Mitra,¹ H. Miyake,⁵³
 S. Moed,²⁰ N. Moggi,⁶ M.N. Mondragon^{k,15} C.S. Moon,²⁵ R. Moore,¹⁵ M.J. Morello,¹⁵
 J. Morlock,²⁴ P. Movilla Fernandez,¹⁵ A. Mukherjee,¹⁵ Th. Muller,²⁴ P. Murat,¹⁵
 M. Mussini^{aa,6} J. Nachtman^{m,15} Y. Nagai,⁵³ J. Naganoma,⁵⁶ I. Nakano,³⁸ A. Napier,⁵⁴
 J. Nett,⁵¹ C. Neu,⁵⁵ M.S. Neubauer,²² J. Nielsen^{d,26} L. Nodulman,² O. Norniella,²²
 E. Nurse,²⁸ L. Oakes,⁴⁰ S.H. Oh,¹⁴ Y.D. Oh,²⁵ I. Oksuzian,⁵⁵ T. Okusawa,³⁹ R. Orava,²¹

L. Ortolan,⁴ S. Pagan Griso^{bb,41} C. Pagliarone,⁵² E. Palencia^{e,9} V. Papadimitriou,¹⁵
 A.A. Paramonov,² J. Patrick,¹⁵ G. Pauletta^{gg,52} M. Paulini,¹⁰ C. Paus,³⁰ D.E. Pellett,⁷
 A. Penzo,⁵² G. Perez^{z,31} T.J. Phillips,¹⁴ G. Piacentino,⁴⁴ E. Pianori,⁴³ J. Pilot,³⁷ K. Pitts,²²
 C. Plager,⁸ L. Pondrom,⁵⁸ K. Potamianos,⁴⁶ O. Poukhov,¹³ F. Prokoshin^{y,13} A. Pronko,¹⁵
 F. Ptohos^{g,17} E. Pueschel,¹⁰ G. Punzi^{cc,44} J. Pursley,⁵⁸ A. Rahaman,⁴⁵ V. Ramakrishnan,⁵⁸
 N. Ranjan,⁴⁶ I. Redondo,²⁹ P. Renton,⁴⁰ M. Rescigno,⁴⁹ T. Riddick,²⁸ F. Rimondi^{aa,6}
 L. Ristori^{44,15} A. Robson,¹⁹ T. Rodrigo,⁹ T. Rodriguez,⁴³ E. Rogers,²² S. Rolli^{h,54}
 R. Roser,¹⁵ M. Rossi,⁵² F. Rubbo,¹⁵ F. Ruffini^{dd,44} A. Ruiz,⁹ J. Russ,¹⁰ V. Rusu,¹⁵
 A. Safonov,⁵¹ W.K. Sakumoto,⁴⁷ Y. Sakurai,⁵⁶ L. Santi^{gg,52} L. Sartori,⁴⁴ K. Sato,⁵³
 V. Saveliev^{u,42} A. Savoy-Navarro,⁴² P. Schlabach,¹⁵ A. Schmidt,²⁴ E.E. Schmidt,¹⁵
 M.P. Schmidt,⁵⁹ M. Schmitt,³⁶ T. Schwarz,⁷ L. Scodellaro,⁹ A. Scribano^{dd,44} F. Scuri,⁴⁴
 A. Sedov,⁴⁶ S. Seidel,³⁵ Y. Seiya,³⁹ A. Semenov,¹³ F. Sforza^{cc,44} A. Sfyrla,²² S.Z. Shalhout,⁷
 T. Shears,²⁷ P.F. Shepard,⁴⁵ M. Shimojima^{t,53} S. Shiraishi,¹¹ M. Shochet,¹¹
 I. Shreyber,³⁴ A. Simonenko,¹³ P. Sinervo,³¹ A. Sissakian,¹³ K. Sliwa,⁵⁴ J.R. Smith,⁷
 F.D. Snider,¹⁵ A. Soha,¹⁵ S. Somalwar,⁵⁰ V. Sorin,⁴ P. Squillacioti,⁴⁴ M. Stancari,¹⁵
 M. Stanitzki,⁵⁹ R. St. Denis,¹⁹ B. Stelzer,³¹ O. Stelzer-Chilton,³¹ D. Stentz,³⁶
 J. Strologas,³⁵ G.L. Strycker,³² Y. Sudo,⁵³ A. Sukhanov,¹⁶ I. Suslov,¹³ K. Takemasa,⁵³
 Y. Takeuchi,⁵³ J. Tang,¹¹ M. Tecchio,³² P.K. Teng,¹ J. Thom^{f,15} J. Thome,¹⁰
 G.A. Thompson,²² E. Thomson,⁴³ P. Ttito-Guzmán,²⁹ S. Tkaczyk,¹⁵ D. Toback,⁵¹
 S. Tokar,¹² K. Tollefson,³³ T. Tomura,⁵³ D. Tonelli,¹⁵ S. Torre,¹⁷ D. Torretta,¹⁵ P. Totaro,⁴¹
 M. Trovato^{ee,44} Y. Tu,⁴³ F. Ukegawa,⁵³ S. Uozumi,²⁵ A. Varganov,³² F. Vázquez^{k,16}
 G. Velev,¹⁵ C. Vellidis,³ M. Vidal,²⁹ I. Vila,⁹ R. Vilar,⁹ J. Vizán,⁹ M. Vogel,³⁵
 G. Volpi^{cc,44} P. Wagner,⁴³ R.L. Wagner,¹⁵ T. Wakisaka,³⁹ R. Wallny,⁸ S.M. Wang,¹
 A. Warburton,³¹ D. Waters,²⁸ M. Weinberger,⁵¹ W.C. Wester III,¹⁵ B. Whitehouse,⁵⁴
 D. Whiteson^{b,43} A.B. Wicklund,² E. Wicklund,¹⁵ S. Wilbur,¹¹ F. Wick,²⁴ H.H. Williams,⁴³
 J.S. Wilson,³⁷ P. Wilson,¹⁵ B.L. Winer,³⁷ P. Wittich^{g,15} S. Wolbers,¹⁵ H. Wolfe,³⁷
 T. Wright,³² X. Wu,¹⁸ Z. Wu,⁵ K. Yamamoto,³⁹ J. Yamaoka,¹⁴ T. Yang,¹⁵ U.K. Yang^{p,11}
 Y.C. Yang,²⁵ W.-M. Yao,²⁶ G.P. Yeh,¹⁵ K. Yi^{m,15} J. Yoh,¹⁵ K. Yorita,⁵⁶ T. Yoshida^{j,39}
 G.B. Yu,¹⁴ I. Yu,²⁵ S.S. Yu,¹⁵ J.C. Yun,¹⁵ A. Zanetti,⁵² Y. Zeng,¹⁴ and S. Zucchelli^{aa6}

(CDF Collaboration)[†]

- ¹*Institute of Physics, Academia Sinica,
Taipei, Taiwan 11529, Republic of China*
- ²*Argonne National Laboratory, Argonne, Illinois 60439, USA*
- ³*University of Athens, 157 71 Athens, Greece*
- ⁴*Institut de Fisica d'Altes Energies, ICREA,
Universitat Autònoma de Barcelona,
E-08193, Bellaterra (Barcelona), Spain*
- ⁵*Baylor University, Waco, Texas 76798, USA*
- ⁶*Istituto Nazionale di Fisica Nucleare Bologna,
^{aa}University of Bologna, I-40127 Bologna, Italy*
- ⁷*University of California, Davis, Davis, California 95616, USA*
- ⁸*University of California, Los Angeles,
Los Angeles, California 90024, USA*
- ⁹*Instituto de Fisica de Cantabria, CSIC-University of Cantabria, 39005 Santander, Spain*
- ¹⁰*Carnegie Mellon University, Pittsburgh, Pennsylvania 15213, USA*
- ¹¹*Enrico Fermi Institute, University of Chicago, Chicago, Illinois 60637, USA*
- ¹²*Comenius University, 842 48 Bratislava,
Slovakia; Institute of Experimental Physics, 040 01 Kosice, Slovakia*
- ¹³*Joint Institute for Nuclear Research, RU-141980 Dubna, Russia*
- ¹⁴*Duke University, Durham, North Carolina 27708, USA*
- ¹⁵*Fermi National Accelerator Laboratory, Batavia, Illinois 60510, USA*
- ¹⁶*University of Florida, Gainesville, Florida 32611, USA*
- ¹⁷*Laboratori Nazionali di Frascati, Istituto Nazionale
di Fisica Nucleare, I-00044 Frascati, Italy*
- ¹⁸*University of Geneva, CH-1211 Geneva 4, Switzerland*
- ¹⁹*Glasgow University, Glasgow G12 8QQ, United Kingdom*
- ²⁰*Harvard University, Cambridge, Massachusetts 02138, USA*
- ²¹*Division of High Energy Physics, Department of Physics,
University of Helsinki and Helsinki Institute of Physics, FIN-00014, Helsinki, Finland*
- ²²*University of Illinois, Urbana, Illinois 61801, USA*
- ²³*The Johns Hopkins University, Baltimore, Maryland 21218, USA*

- ²⁴*Institut für Experimentelle Kernphysik,
Karlsruhe Institute of Technology, D-76131 Karlsruhe, Germany*
- ²⁵*Center for High Energy Physics: Kyungpook National University,
Daegu 702-701, Korea; Seoul National University, Seoul 151-742,
Korea; Sungkyunkwan University, Suwon 440-746,
Korea; Korea Institute of Science and Technology Information,
Daejeon 305-806, Korea; Chonnam National University, Gwangju 500-757,
Korea; Chonbuk National University, Jeonju 561-756, Korea*
- ²⁶*Ernest Orlando Lawrence Berkeley National Laboratory, Berkeley, California 94720, USA*
- ²⁷*University of Liverpool, Liverpool L69 7ZE, United Kingdom*
- ²⁸*University College London, London WC1E 6BT, United Kingdom*
- ²⁹*Centro de Investigaciones Energeticas
Medioambientales y Tecnologicas, E-28040 Madrid, Spain*
- ³⁰*Massachusetts Institute of Technology,
Cambridge, Massachusetts 02139, USA*
- ³¹*Institute of Particle Physics: McGill University, Montréal,
Québec, Canada H3A 2T8; Simon Fraser University, Burnaby,
British Columbia, Canada V5A 1S6; University of Toronto,
Toronto, Ontario, Canada M5S 1A7; and TRIUMF,
Vancouver, British Columbia, Canada V6T 2A3*
- ³²*University of Michigan, Ann Arbor, Michigan 48109, USA*
- ³³*Michigan State University, East Lansing, Michigan 48824, USA*
- ³⁴*Institution for Theoretical and Experimental Physics, ITEP, Moscow 117259, Russia*
- ³⁵*University of New Mexico, Albuquerque, New Mexico 87131, USA*
- ³⁶*Northwestern University, Evanston, Illinois 60208, USA*
- ³⁷*The Ohio State University, Columbus, Ohio 43210, USA*
- ³⁸*Okayama University, Okayama 700-8530, Japan*
- ³⁹*Osaka City University, Osaka 588, Japan*
- ⁴⁰*University of Oxford, Oxford OX1 3RH, United Kingdom*
- ⁴¹*Istituto Nazionale di Fisica Nucleare, Sezione di Padova-Trento,
^{bb}University of Padova, I-35131 Padova, Italy*
- ⁴²*LPNHE, Universite Pierre et Marie*

Curie/IN2P3-CNRS, UMR7585, Paris, F-75252 France

⁴³*University of Pennsylvania, Philadelphia, Pennsylvania 19104, USA*

⁴⁴*Istituto Nazionale di Fisica Nucleare Pisa, ^{cc}University of Pisa,*

^{dd}*University of Siena and ^{ee}Scuola Normale Superiore, I-56127 Pisa, Italy*

⁴⁵*University of Pittsburgh, Pittsburgh, Pennsylvania 15260, USA*

⁴⁶*Purdue University, West Lafayette, Indiana 47907, USA*

⁴⁷*University of Rochester, Rochester, New York 14627, USA*

⁴⁸*The Rockefeller University, New York, New York 10065, USA*

⁴⁹*Istituto Nazionale di Fisica Nucleare, Sezione di Roma 1,*

^{ff}*Sapienza Università di Roma, I-00185 Roma, Italy*

⁵⁰*Rutgers University, Piscataway, New Jersey 08855, USA*

⁵¹*Texas A&M University, College Station, Texas 77843, USA*

⁵²*Istituto Nazionale di Fisica Nucleare Trieste/Udine,*

I-34100 Trieste, ^{gg}University of Udine, I-33100 Udine, Italy

⁵³*University of Tsukuba, Tsukuba, Ibaraki 305, Japan*

⁵⁴*Tufts University, Medford, Massachusetts 02155, USA*

⁵⁵*University of Virginia, Charlottesville, Virginia 22906, USA*

⁵⁶*Waseda University, Tokyo 169, Japan*

⁵⁷*Wayne State University, Detroit, Michigan 48201, USA*

⁵⁸*University of Wisconsin, Madison, Wisconsin 53706, USA*

⁵⁹*Yale University, New Haven, Connecticut 06520, USA*

Abstract

A study of the substructure of jets with transverse momentum greater than 400 GeV/ c produced in proton-antiproton collisions at a center-of-mass energy of 1.96 TeV at the Fermilab Tevatron Collider and recorded by the CDF II detector is presented. The distributions of the jet mass, angularity, and planar flow are measured for the first time in a sample with an integrated luminosity of 5.95 fb⁻¹. The observed substructure for high mass jets is consistent with predictions from perturbative quantum chromodynamics.

PACS numbers: 12.38.Qk, 13.87.-a, 14.65.Ha, 12.38.Aw

[†] With visitors from ^aIstituto Nazionale di Fisica Nucleare, Sezione di Cagliari, 09042 Monserrato (Cagliari),

Italy, ^bUniversity of CA Irvine, Irvine, CA 92697, USA, ^cUniversity of CA Santa Barbara, Santa Barbara, CA 93106, USA, ^dUniversity of CA Santa Cruz, Santa Cruz, CA 95064, USA, ^eCERN, CH-1211 Geneva, Switzerland, ^fCornell University, Ithaca, NY 14853, USA, ^gUniversity of Cyprus, Nicosia CY-1678, Cyprus, ^hOffice of Science, U.S. Department of Energy, Washington, DC 20585, USA, ⁱUniversity College Dublin, Dublin 4, Ireland, ^jUniversity of Fukui, Fukui City, Fukui Prefecture, Japan 910-0017, ^kUniversidad Iberoamericana, Mexico D.F., Mexico, ^lIowa State University, Ames, IA 50011, USA, ^mUniversity of Iowa, Iowa City, IA 52242, USA, ⁿKinki University, Higashi-Osaka City, Japan 577-8502, ^oKansas State University, Manhattan, KS 66506, USA, ^pUniversity of Manchester, Manchester M13 9PL, United Kingdom, ^qQueen Mary, University of London, London, E1 4NS, United Kingdom, ^rUniversity of Melbourne, Victoria 3010, Australia, ^sMuons, Inc., Batavia, IL 60510, USA, ^tNagasaki Institute of Applied Science, Nagasaki, Japan, ^uNational Research Nuclear University, Moscow, Russia, ^vUniversity of Notre Dame, Notre Dame, IN 46556, USA, ^wUniversidad de Oviedo, E-33007 Oviedo, Spain, ^xTexas Tech University, Lubbock, TX 79609, USA, ^yUniversidad Tecnica Federico Santa Maria, 110v Valparaiso, Chile, ^zWeizmann Institute of Science, Rehovot, Israel, ^{aa}Yarmouk University, Irbid 211-63, Jordan, ^{hh}On leave from J. Stefan Institute, Ljubljana, Slovenia,

The study of high transverse momentum (p_T) massive jets produced in proton-antiproton ($p\bar{p}$) interactions provides an important test of perturbative QCD (pQCD) and gives insight into the parton showering mechanism (see e.g., [1, 2] for recent reviews). Furthermore, massive boosted jets constitute an important background in searches for various new physics models [3–6], the Higgs boson [7], and highly boosted top quark production. Particularly relevant is the case where the decay of a heavy resonance produces high- p_T top quarks that decay hadronically. In all these cases, the hadronic decay products can be detected as a single jet with a large mass and internal substructure that differs on average from pQCD jets once the jet p_T is greater than 400-500 GeV/ c . However, experimental studies of the substructure of high p_T jets at the Tevatron have been limited to jets with $p_T < 400$ GeV/ c [8, 9]; recently results with higher p_T jets produced at the Large Hadron Collider have been published [10].

Jets produced through QCD processes with large mass are expected to arise predominantly through a process of single hard gluon emission from a high p_T quark or gluon [11]. The probability of this process is given by the jet function, $J(m^{jet}, p_T, R)$, for which a simple next-to-leading-order (NLO) approximation is

$$J(m^{jet}, p_T, R) \simeq \alpha_s(p_T) \frac{4 C_{q,g}}{\pi m^{jet}} \log \left(\frac{R \cdot p_T}{m^{jet}} \right), \quad (1)$$

where m^{jet} is the jet mass, $\alpha_s(p_T)$ is the strong coupling, $C_{q,g} = 4/3$ and 3 for quark and gluon jets, respectively, and R is the cone radius used to define the jet [11]. The approximation holds for $m^{jet} \ll R \cdot p_T$. Although uncertainties from higher-order corrections are $\sim 30\%$, it predicts both the shape of the spectrum and the fraction of jets with masses greater than about 100 GeV/ c^2 . Two other jet substructure variables insensitive to soft radiation at high jet mass are angularity and planar flow [12–16]. The angularity is defined as

$$\tau_{-2}(R, p_T) \equiv \frac{1}{m^{jet}} \sum_{i \in jet} E_i \sin^{-2} \theta_i [1 - \cos \theta_i]^3, \quad (2)$$

where the sum is over the constituents in the jet cluster, E_i is the energy and θ_i is the angle of each constituent relative to the jet axis. It is sensitive to radiation near the edge of the cone and has a characteristic shape for QCD jets. Planar flow is defined as

$$Pf \equiv \frac{4\lambda_1\lambda_2}{(\lambda_1 + \lambda_2)^2}, \quad (3)$$

where $\lambda_{1,2}$ are the eigenvalues of the two-dimensional moment matrix

$$I_w^{kl} = \frac{1}{m^{jet}} \sum_{i \in jet} E_i \frac{p_{i,k}}{E_i} \frac{p_{i,l}}{E_i}, \quad (4)$$

in which $p_{i,k}$ is the k^{th} component of the jet constituent's transverse energy relative to the jet axis, *i.e.* in one of the two directions that span the plane perpendicular to the jet direction. Jets with three or more energetic constituents, such as those arising from a boosted top quark, are more planar with $Pf \sim 1$, compared with massive QCD jets where the energy flow is along the line defined by the two final-state partons and $Pf \sim 0$. Both of these variables are perturbatively calculable.

We report in this Letter the first measurement of the jet mass distribution for jets with $p_T > 400$ GeV/ c produced in 1.96 TeV $p\bar{p}$ collisions at the Fermilab Tevatron Collider and recorded by the CDF II detector. We also measure for jets with masses greater than 90 GeV/ c^2 their angularity and planar flow distributions. We use the Midpoint cone algorithm [17] to reconstruct jets using the FASTJET program [18] and the *anti- k_t* algorithm [19], allowing for a direct comparison of cone and recombination algorithms.

The CDF II detector [20] consists of a solenoidal charged particle spectrometer surrounded by a calorimeter and muon system. Charged particle momenta are measured over $|\eta| < 1.1$. The calorimeter covers the region $|\eta| < 3.6$, with the region $|\eta| < 1.1$ segmented into towers of size $\Delta\eta \times \Delta\phi = 0.11 \times 0.26$ [21]. The calorimeter system is used to measure jets and missing transverse energy (\cancel{E}_T) defined as

$$\vec{\cancel{E}}_T = - \sum_i E_T^i \hat{n}_i, \quad (5)$$

where the sum is over the calorimeter towers with $|\eta| < 3.6$ and \hat{n}_i is a unit vector perpendicular to the beam axis and pointing at the i^{th} calorimeter tower. We also define $\cancel{E}_T = |\vec{\cancel{E}}_T|$. The 4-momentum of a jet is the sum over the calorimeter towers in the jet, where each calorimeter tower is treated as a massless 4-vector, and the jet mass is obtained from the resulting 4-vector.

We select events in a sample with 5.95 fb $^{-1}$ integrated luminosity identified with an inclusive jet trigger requiring at least one jet with transverse energy (E_T) > 100 GeV, with the trigger becoming fully efficient for jets with $E_T > 140$ GeV. Jet candidates are constructed with a Midpoint cone algorithm with cone radii of $R = 0.4$ and 0.7 and with the *anti- k_t* algorithm with a distance parameter $R = 0.7$. Primary collision vertices are reconstructed using charged particle information. Events are required to have at least one high quality primary vertex with $|z_{vtx}| < 60$ cm. Events are also required to be well-measured by requiring that they satisfy a missing transverse energy significance requirement

of $S_{MET} < 10 \text{ GeV}^{1/2}$, defined as

$$S_{MET} \equiv \frac{\cancel{E}_T}{\sqrt{\sum E_T}}, \quad (6)$$

where the sum is over all calorimeter towers. We calculate for each jet the scalar sum of the p_T of the tracks associated with the jet cluster. Each jet is required to either have more than 5% of its energy registered in the electromagnetic calorimeter or to have its summed track momentum be at least 5%. This criterion eliminates jet candidates arising from instrumental backgrounds. Furthermore, we restrict the jet candidates to have $0.1 < |\eta_d| < 0.7$, where η_d is the jet pseudorapidity in the detector frame of reference, to ensure optimal calorimeter and charged particle tracking coverage. The minimum pseudo rapidity requirement avoids a region of the calorimeter where the energy response is varying rapidly. We further require that the leading jet in the event have $p_T > 400 \text{ GeV}/c$. We observe 2699 events.

The jet 4-momentum is corrected to take into account calorimeter energy response, which is known to a precision of 3% [22] for central calorimeter jets with $p_T > 400 \text{ GeV}/c$. We have determined the uncertainty on calibration of the jet mass measurement by comparing the momentum flux of charged particles into three concentric regions of the calorimeter around the jet centroid with the corresponding calorimeter response.

The number of interaction vertices (N_{vtx}) is a measure of the number of multiple interactions (MI), *i.e.* additional collisions in the same bunch crossing, and averages ~ 3 in this sample. We make a data-driven correction for MI effects on the jet substructure variables [23]. To calculate these corrections, we select a subset of events with a back-to-back dijet topology. We then define cones at right angles to the leading jet in azimuth of the same size as the jet cluster, and add the calorimeter towers in these cones to the jet 4-vector after rotation by 90° into the jet cone. The resulting average mass shift upward as a function of m^{jet} is taken as the correction downward due to MI and the energy flow from the underlying event (UE) of the hard collision. We separately measure the UE correction by using only events with $N_{\text{vtx}} = 1$. We correct the leading jet mass, m^{jet1} , for events with $N_{\text{vtx}} > 1$ by the difference between the mass shift in multi-vertex events and the mass shift in single vertex events. The correction has an approximate $1/m^{jet1}$ behaviour and averages $\sim 4 \text{ GeV}/c^2$ for a jet cone size of $R = 0.7$. The jet mass correction for a cone size of $R = 0.4$ is $\sim 0.5 \text{ GeV}/c^2$, consistent with the expected R^4 scaling [2]. In the following, we focus on results for $R = 0.7$ Midpoint jets.

To model the high p_T processes, we used a PYTHIA 6.216 calculation [16] of QCD jet production generated with parton $\hat{p}_T > 300$ GeV/ c , using the Tune A [24] parameters for the underlying event and the CTEQ5L parton distribution functions (PDFs), followed by a full detector simulation. Based on a PYTHIA calculation, we estimate W and Z boson production to contribute ~ 25 jets with masses between 60 and 100 GeV/ c^2 , which is less than 5% of the number observed. However, top quark pair production can contribute to the jet mass region $m^{jet1} > 100$ GeV/ c^2 where the expected QCD jet rate is much lower. We employ an approximate next-to-next-to-leading order (NNLO) calculation of the $t\bar{t}$ differential cross section [25] updated with the MSTW 2008 PDFs [26] and a top quark mass of $m_{top} = 173$ GeV/ c^2 [27]. This yields a cross section for top quark jets with $p_T > 400$ GeV/ c of 4.6 fb. We used the PYTHIA 6.216 generator to create a $t\bar{t}$ MC sample and applied the same selection requirements used to define the event sample. The estimated $t\bar{t}$ contribution to the data sample, normalized to the NNLO cross section, is 13 ± 4 events.

Two-thirds of the $t\bar{t}$ events with a leading high p_T jet would produce a recoil jet with a large jet mass (m^{jet2}) arising from the fully-hadronic decay of the recoil top quark. The remaining $t\bar{t}$ events would have a recoil top quark that decays semileptonically, resulting in large \cancel{E}_T and a recoil jet with lower p_T and m^{jet2} . We reduce these backgrounds by rejecting events with $m^{jet2} > 100$ GeV/ c^2 or by making a more stringent \cancel{E}_T requirement by rejecting events with $S_{MET} > 4$ GeV $^{1/2}$. Approximately 25% (80%) of the $t\bar{t}$ (QCD) MC events survive these requirements. We observe 30 jets with $m^{jet} > 140$ GeV/ c^2 and expect a $t\bar{t}$ contribution of at most three jets.

In order to compare our results with QCD predictions, we correct the m^{jet} distributions for effects of selection and resolution by an unfolding procedure, where we correct bin-by-bin the observed m^{jet1} distribution by the ratio of the QCD PYTHIA MC m^{jet1} distribution without detector effects and the same distribution after measurement and selection effects have been included. This jet mass unfolding correction was derived for each jet algorithm separately, and the correction factors vary from 1.6 to 2.0 over the jet mass range > 70 GeV/ c^2 . These corrections were verified through studies of the data and confirmed with MC calculations.

We summarize briefly our estimates of the systematic uncertainties that affect the substructure observables. The overall jet mass scale at these energies is known to 2 (10) GeV/ c^2 for jet masses of 60 (120) GeV/ c^2 , based on the jet energy scale uncertainty and the comparison of the calorimeter energy and track momentum measurements within the jet mentioned

above. We assign an uncertainty on the MI correction of $2 \text{ GeV}/c^2$, which is half of the average correction. We assign a $\sim 15\%$ uncertainty on the jet mass unfolding correction due to modeling of the jet hadronization, the uncertainty arising from the selection, and MC statistical uncertainties. The hadronization uncertainty is conservatively determined by comparing the change in the correction when hadronization is turned off in the MC samples. We estimate the PDF uncertainties on the PYTHIA predictions by reweighting the MC events using the $\pm 1\sigma$ variations in the 20 eigenvectors describing the uncertainties in the PDFs [28]; the uncertainties on the jet mass, angularity and planar flow distributions are 10% or less in all cases.

We show in Fig. 1 a comparison of the unfolded m^{jet1} distribution for a cone size $R = 0.7$ with the analytic predictions for the jet function. This comparison, made for jet masses above $70 \text{ GeV}/c^2$, shows that the analytical prediction for quark jets describes approximately the shape of the distribution and fraction of jets but tends to over-estimate the rate for jet masses from 130 to $200 \text{ GeV}/c^2$. The better agreement of the quark jet function with data compared with that of the gluon is consistent with the pQCD prediction that $\sim 80\%$ of these jets arise from quarks [29], though we emphasize that the uncertainties of the pQCD predictions are large. Furthermore, the data and the PYTHIA distributions are in reasonable agreement. We also compare in the inset figure the distributions obtained for the Midpoint and *anti- k_t* algorithms. The *anti- k_t* jets have a similar mass distribution to the Midpoint jets. The *anti- k_t* algorithm, however, does not produce as large a tail of very massive jets, presumably due to the lack of an explicit merging mechanism. This difference in algorithm performance is reproduced by the PYTHIA calculation. We find that $1.4 \pm 0.3\%$ of the Midpoint jets with $p_T > 400 \text{ GeV}/c$ have $m^{jet1} > 140 \text{ GeV}/c^2$. This is the first measurement of this rate, and allows us to constrain QCD predictions of this fraction, and provide the first measurement of the rate of backgrounds in a massive jet sample from QCD production of high p_T light quarks and gluons.

A key prediction of the NLO QCD calculation is that the distribution of angularities [12, 13] of high mass jets has relatively sharp kinematical edges, with minimum and maximum values given by

$$\tau_{-2}^{\min} \sim (2/z)^{-3}, \tau_{-2}^{\max} \sim zR^2/2^3, \quad (7)$$

with $z \equiv m^{jet}/p_T$. We show in Fig. 2 the angularity distribution for the leading jet requiring that $m^{jet1} \in (90, 120) \text{ GeV}/c^2$. The requirement of a relatively narrow m^{jet1} window allows

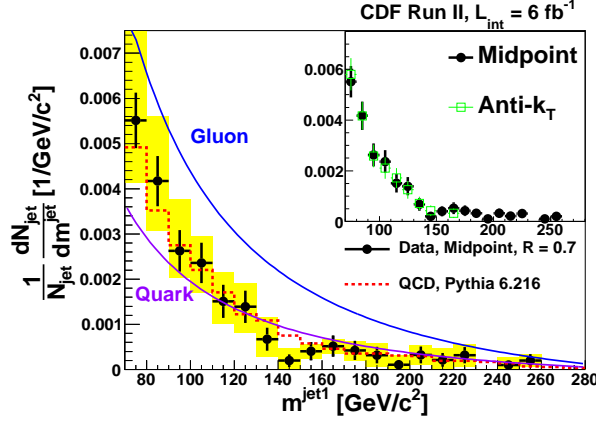


FIG. 1. The normalized jet mass distribution for Midpoint jets with $p_T > 400$ GeV/ c and $|\eta| \in (0.1, 0.7)$. The uncertainties shown are statistical (black lines) and systematic (yellow bars). The theory predictions for the jet function for quarks and gluons are shown as solid curves and have an estimated uncertainty of $\sim 30\%$. We also show the PYTHIA MC prediction (red dashed line). The inset compares Midpoint (full black circles) and $anti-k_t$ (open green squares) jets.

us to compare the observed distribution with the shape and kinematic endpoints predicted by pQCD. The PYTHIA and pQCD predictions are in good agreement with the data for Midpoint and $anti-k_t$ jets, although the small size of the jet sample after applying the mass criterion limits the statistical precision of the comparison. This further strengthens the interpretation that these massive jets arise from two-body configurations. The small number of jets below τ_{-2}^{\min} arise from resolution effects. The PDF uncertainties on the PYTHIA predictions are 10%, and are shown in the figure. The results for jets with cone sizes of $R = 0.4$ are similar.

Figure 3 shows the planar flow distribution for jets where the jet mass is required to be in the range $130 - 210$ GeV/ c^2 , relevant for jets arising from top quark decays. Comparisons with the PYTHIA predictions are also shown for both QCD multi-jet and $t\bar{t}$ production. Although the data are in good agreement with the predictions from QCD, the comparison is statistically limited because of the small number of observed jets in this jet mass range. The PDF uncertainties on the PYTHIA QCD predictions are 10%. The results for jets reconstructed with the Midpoint and $anti-k_t$ algorithms are in good agreement with each other and are consistent with the general expectation based on MC calculations [11]. This study suggests that with higher statistics it will be possible to use the planar flow variable to discriminate high p_T QCD and top quark jets independent of jet mass.

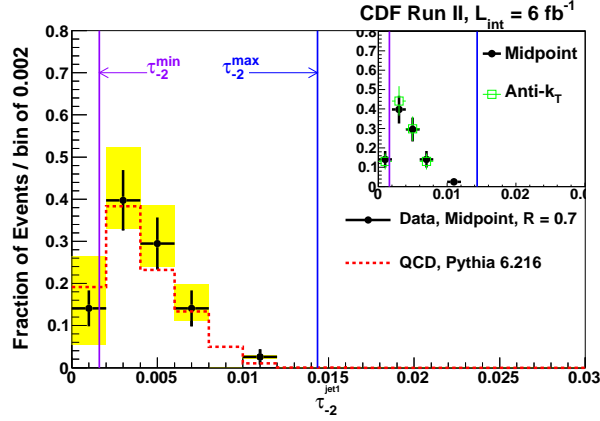


FIG. 2. The angularity distribution for Midpoint jets with $p_T > 400$ GeV/ c and $|\eta| \in (0.1, 0.7)$. We have applied cuts to reject $t\bar{t}$ events and required that $m^{jet1} \in (90, 120)$ GeV/ c^2 . We also show the PYTHIA calculation (red dashed line) and the pQCD kinematic endpoints. The inset compares the distributions for Midpoint (full black circles) and $anti-k_t$ (open green squares) jets.

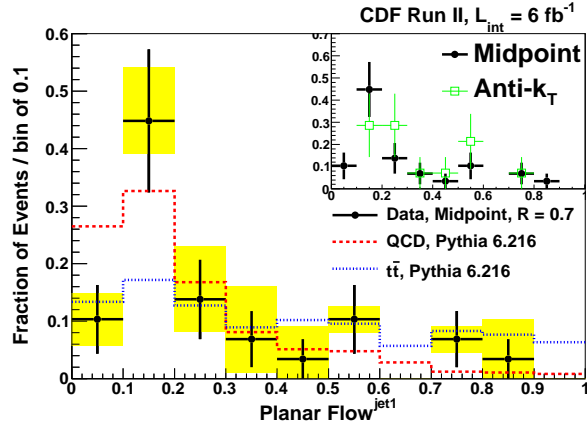


FIG. 3. The planar flow distributions for Midpoint jets with $p_T > 400$ GeV/ c and $|\eta| \in (0.1, 0.7)$ after applying the top rejection cuts and requiring $m^{jet1} \in (130, 210)$ GeV/ c^2 . We also show the PYTHIA QCD (red dashed line) and $t\bar{t}$ (blue dotted line) jets, as well as the results from the two jet algorithms (inset). All distributions have been separately normalized to unity. We expect only $\sim 10\%$ of the jets to arise from SM $t\bar{t}$ production.

In summary, we have measured for the first time the mass, angularity and planar flow distributions for jets with $p_T > 400$ GeV/ c using Midpoint and $anti-k_t$ jet algorithms. We find good agreement between PYTHIA Monte Carlo predictions, the NLO QCD jet function predictions, and the data for the jet mass distribution above 100 GeV/ c^2 for Midpoint

and *anti- k_t* jets. The Midpoint and *anti- k_t* algorithms have very similar jet substructure distributions for high mass jets. Our results show that the use of jet mass is an effective variable for separation of jets produced through QCD and through $t\bar{t}$ production, with a jet mass requirement of greater than $140 \text{ GeV}/c^2$ leaving only $1.4 \pm 0.3\%$ of the QCD jets. We have also shown that the high mass jets coming from light quark and gluon production are consistent with two-body final states from a study of the angularity variable, and that it may be possible to use the planar flow variable to further reject high mass QCD jets. These results provide the first experimental evidence that validates the MC calculations employing jet substructure to search for exotic heavy particles.

ACKNOWLEDGMENTS

We acknowledge the contributions of I. Sung and G. Sterman for discussions involving non-perturbative effects in QCD jets, and to N. Kidonakis for updated top quark differential cross section calculations.

We thank the Fermilab staff and the technical staffs of the participating institutions for their vital contributions. This work was supported by the U.S. Department of Energy and National Science Foundation; the Italian Istituto Nazionale di Fisica Nucleare; the Ministry of Education, Culture, Sports, Science and Technology of Japan; the Natural Sciences and Engineering Research Council of Canada; the National Science Council of the Republic of China; the Swiss National Science Foundation; the A.P. Sloan Foundation; the Bundesministerium für Bildung und Forschung, Germany; the Korean World Class University Program, the National Research Foundation of Korea; the Science and Technology Facilities Council and the Royal Society, UK; the Institut National de Physique Nucleaire et Physique des Particules/CNRS; the Russian Foundation for Basic Research; the Ministerio de Ciencia e Innovación, and Programa Consolider-Ingenio 2010, Spain; the Slovak R&D Agency; the Academy of Finland; and the Australian Research Council (ARC).

This work was supported in part by a grant from the Shrum Foundation, and by the

- [1] S. D. Ellis, J. Huston, K. Hatakeyama, P. Loch, and M. Toennesmann, *Prog. Part. Nucl. Phys.* **60**, 484 (2008), arXiv:hep-ph/0712.2447.
- [2] G. P. Salam, *Eur. Phys. J.* **67**, 637 (2010), arXiv:hep-ph/0906.1833.
- [3] .
- [4] K. Agashe, A. Belyaev, T. Krupovnickas, G. Perez, and J. Virzi, *Phys. Rev. D* **77**, 015003 (2008), arXiv:hep-ph/0612015.
- [5] B. Lillie, L. Randall, and L. T. Wang, *JHEP* **0709**, 074 (2007), arXiv:hep-ph/0701166.
- [6] J. M. Butterworth, J. R. Ellis, A. R. Raklev, and G. P. Salam, *Phys. Rev. Lett.* **103**, 241803 (2009), arXiv:hep-ph/0906.0728.
- [7] J. M. Butterworth, A. R. Davison, M. Rubin, and G. P. Salam, *Phys. Rev. Lett.* **100**, 242001 (2008), arXiv:hep-ph/0802.2470.
- [8] V. M. Abazov *et al.* (D0 Collaboration), *Phys. Rev. D* **65**, 052008 (2002), arXiv:hep-ex/0108054.
- [9] D. Acosta *et al.* (CDF Collaboration), *Phys. Rev. D* **71**, 112002 (2005), arXiv:hep-ex/0505013.
- [10] G. Aad *et al.* (ATLAS Collaboration), *Phys. Rev. D* **83**, 052003 (2011), arXiv:1101.0070 [hep-ex].
- [11] L. G. Almeida, S. J. Lee, G. Perez, I. Sung, and J. Virzi, *Phys. Rev. D* **79**, 074012 (2009), arXiv:hep-ph/0810.0934.
- [12] C. F. Berger, T. Kucs, and G. Sterman, *Phys. Rev. D* **68**, 014012 (2003), arXiv:hep-ph/0303051.
- [13] L. G. Almeida, S. J. Lee, G. Perez, G. Sterman, I. Sung, and J. Virzi, *Phys. Rev. D* **79**, 074017 (2009), arXiv:hep-ph/0807.0234.
- [14] S. D. Ellis, C. K. Vermilion, J. R. Walsh, A. Hornig, and C. Lee, *JHEP* **1011**, 101 (2010), arXiv:hep-ph/1001.0014.
- [15] J. Thaler and L. T. Wang, *JHEP* **0807**, 092 (2008), arXiv:hep-ph/0806.0023.
- [16] T. Sjostrand, S. Mrenna, and P. Z. Skands, *JHEP* **05**, 026 (2006), arXiv:hep-ph/0603175.
- [17] G. C. Blazey *et al.*, arXiv:hep-ex/0005012.
- [18] M. Cacciari and G. P. Salam, *Phys. Lett. B* **641**, 57 (2006), arXiv:hep-ph/0512210.

- [19] M. Cacciari, G. P. Salam, and G. Soyez, JHEP **04**, 063 (2008), arXiv:0802.1189.
- [20] D. Acosta *et al.* (CDF Collaboration), Phys. Rev. D **71**, 032001 (2005), arXiv:hep-ex/0412071.
- [21] We use a coordinate system where ϕ and θ are the azimuthal and polar angles around the proton beam axis, which defines the z axis. The origin of the coordinate system is the nominal interaction point in the detector. The pseudorapidity is $\eta = -\ln \tan(\theta/2)$ and $R = \sqrt{(\delta\eta)^2 + (\delta\phi)^2}$.
- [22] A. Bhatti *et al.*, Nucl. Instrum. Methods A **566**, 375 (2006), arXiv:hep-ex/0510047.
- [23] R. Alon, E. Duchovni, G. Perez, A. P. Pranko, and P. Sinervo, Phys. Rev. D **84**, 114025 (2011), arXiv:hep-ph/1101.3002.
- [24] R. Field (CDF and D0 Collaborations), AIP Conference Proceedings **828**, 163 (2006).
- [25] N. Kidonakis and R. Vogt, Phys. Rev. D **68**, 114014 (2003), arXiv:hep-ph/0308222.
- [26] A. D. Martin, W. J. Stirling, R. S. Thorne, and G. Watt, Eur. Phys. J. C **63**, 189 (2009), arXiv:hep-ph/0901.0002.
- [27] N. Kidonakis, personal communication.
- [28] J. Pumplin *et al.*, Phys. Rev. D **65**, 014013 (2001), arXiv:hep-ph/0101032.
- [29] R. K. Ellis, W. J. Stirling, and B. R. Webber, *QCD and Collider Physics* (Cambridge University Press, 1994).